

Microflow-based control of near-wall fluctuations for large viscous drag reduction

Jovan Jovanović · Bettina Frohnafel ·
Rubitha Srikantharajah · Djordje Jovanović ·
Hermann Lienhart · Antonio Delgado

Received: 28 March 2011 / Accepted: 16 June 2011 / Published online: 13 July 2011
© Springer-Verlag 2011

Abstract The stabilizing effect of microgroove surface morphology on viscous drag reduction was studied experimentally in the inlet region of a plane channel flow. The stabilization is thought to be due to the ability of a microgrooved surface pattern to suppress the velocity fluctuations in the spanwise direction on a restricted portion of the wetted surface, which prevents vorticity development at the wall and consequently across the entire flow field. This smart microflow control strategy, which works successfully only under very particular circumstances, was implemented in a microgroove-modified channel flow in which the front part has a microgrooved surface topology. The results of pressure drop measurements indicate that microgrooved surfaces can effectively stabilize laminar boundary layer development, leading to a significant reduction in the viscous drag. In the rear flat part of the microgroove-modified channel test section, a maximum drag reduction of $DR \simeq 35\%$ was measured. This corresponds to an overall drag reduction of $DR \simeq 16\%$ at a length Reynolds number of $Re_x \simeq 10^6$. The drag reduction effect persisted in a narrow range of flow velocities and for the reported experimental conditions corresponds to microgroove dimensions between 1.5 and 2.5 viscous length-scales.

1 Introduction

We have previously shown that a significant reduction in turbulent drag can be obtained by using surface-embedded microgrooves in a fully developed turbulent channel flow (Frohnafel et al. 2007). In a series of experiments, drag reduction was deduced from pressure drop measurements in a microgroove-modified channel flow. Measurements have shown that the magnitude of the drag reduction far exceeds what has been achieved so far but exists only in a narrow range of flow velocities corresponding to microgroove dimensions of less than one viscous length-scale. In the present paper, we show that the same surface pattern that was successfully used for turbulent flow control can also be employed to stabilize the laminar boundary layer development.

Similarities between fully developed turbulence and laminar to turbulence transition and, therefore, between turbulent drag reduction and stabilization of the laminar boundary layer have been reported previously (Hinze 1975; Jovanović et al. 2006; Laufer 1975, 1982). In our previous work, we focused on the importance of energy dissipation for viscous drag reduction and in the following it will be shown how this analysis leads to the conclusion that similar surface structures can be used for both cases, turbulent drag reduction and laminar boundary layer stabilization.

In channel and pipe flows, the average total energy dissipation rate $\bar{\Phi}$:

$$\frac{1}{V} \int_V \underbrace{\left[\underbrace{\nu \left(\frac{\partial \bar{U}_i}{\partial x_j} + \frac{\partial \bar{U}_j}{\partial x_i} \right) \frac{\partial \bar{U}_i}{\partial x_j}}_I + \underbrace{\nu \left(\frac{\partial u_i}{\partial x_j} + \frac{\partial u_j}{\partial x_i} \right) \frac{\partial u_i}{\partial x_j}}_{II} \right]}_{\bar{\Phi}} dV = \frac{A_w \tau_w U_B}{\rho V}, \quad (1)$$

J. Jovanović (✉) · R. Srikantharajah · Dj. Jovanović ·
H. Lienhart · A. Delgado
Institute of Fluid Mechanics, Friedrich-Alexander University
Erlangen-Nuremberg, Cauerstrasse 4, 91058 Erlangen, Germany
e-mail: jovan.jovanovic@lstm.uni-erlangen.de

J. Jovanović · B. Frohnafel
Center of Smart Interfaces, Technische Universität Darmstadt,
Petersenstrasse 32, 64287 Darmstadt, Germany
e-mail: frohnafel@csi.tu-darmstadt.de

is composed of direct (I) and turbulent dissipation (II) and can be evaluated from the work done against the wall shear stress, τ_w , per unit mass of the working fluid, ρV , where A_w is the wetted surface area and U_B is the bulk velocity. An order of magnitude analysis shows that in turbulent flows the largest contribution to $\overline{\Phi}$ is due to turbulent dissipation, ε , which reaches a maximum at the wall, as shown in Fig. 1. Therefore, a large turbulent drag reduction can be expected if the turbulent dissipation at the wall is minimized. It can be shown that kinematic constraints imposed by local axisymmetry on the velocity fluctuations near the wall force the turbulent dissipation rate to vanish at a solid surface (Jovanović et al. 2006). Since near-wall velocity fluctuations are always two-component and the required axisymmetry is in respect to the axis aligned with the flow direction, the resulting near-wall turbulence corresponds to a one-component state with the streamwise velocity component being much larger than in the other two directions.

The examination of numerical databases of wall-bounded flows reveals that whenever turbulence approaches the one-component limit near the wall, such a tendency is accompanied by: (i) an increase in the smallest scale of motion defined in terms of Kolmogorov's length-scale, $\eta_K = (v^3/\varepsilon)^{1/4}$; (ii) a consequent decrease in the spectral separation, L/η_K , which represents the ratio between the large, L , and smallest scale, η_K , of motion; and (iii) a reduction in the turbulent Reynolds number $R_\lambda = q\lambda/\nu$ based on Taylor's micro scale, which is related to ε by $\varepsilon \simeq 5\nu q^2/\lambda^2$. (iii) Conclusion can be drawn since the ratio L/η_K can be solely approximated in terms of R_λ , which decreases as R_λ decreases (Jovanović et al. 2006). These

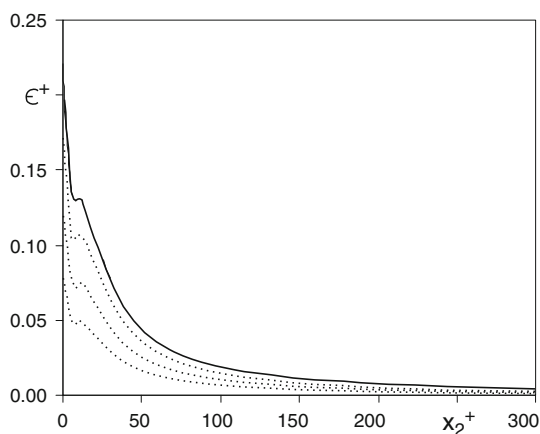


Fig. 1 Distribution of the turbulent dissipation rate versus wall distance normalized with the wall shear velocity and the kinematic viscosity of the flow medium for a plane channel flow. The *solid line* corresponds to the DNS data at $Re_\tau = 395$ (Moser et al. 1999); the *dotted lines* show sketched estimates of ε^+ profiles for decreasing turbulent dissipation at the wall and increasing drag reduction, which reaches a maximum when $\varepsilon_{\text{wall}} \rightarrow 0$.

deductions are in close agreement with the results of direct numerical simulations with forced boundary conditions which display high drag reduction when turbulence in the viscous sublayer is manipulated to tend toward the one-component state in an axisymmetric fashion (Frohnäpfel et al. 2007; Lee and Kim 2002; Satake and Kasagi 1996).

Based on the considerations summarized above, the surface topology for turbulent drag reduction was designed to force turbulence at the wall to tend toward the one-component state by inserting microgrooves (as shown in Fig. 2), which on a restricted part of the wetted surface, suppress velocity fluctuations in the normal and spanwise directions almost to the same extent (Frohnäpfel et al. 2007).

For laminar boundary layer control, a qualitative analysis of the transport equations for statistical properties of small disturbances can provide an interesting insight. Assuming that the disturbances are statistically axisymmetric and neutrally stable so that equilibrium exists between production and viscous dissipation during the period of stable laminar flow development, one deduces that high values of anisotropy in the free stream have a stabilizing effect on the boundary layer development. A comparison of existing experimental data and the theoretical prediction supports this deduction (Jovanović et al. 2006). This analysis is not restricted to the influence of anisotropy in the free stream but in addition includes the behavior of disturbances in the near-wall region. As the wall is approached, $x_2 \rightarrow 0$, the energy of the disturbances, $k = 1/2q^2$, increases as $k \rightarrow (\varepsilon_{\text{wall}}/\nu)x_2^2/2$. If disturbances in the near-wall region are statistically axisymmetric and fixed at the one-component state, the turbulent dissipation at the wall cannot develop ($\varepsilon_{\text{wall}} = 0$) and we may expect that such disturbances cannot be amplified so that the

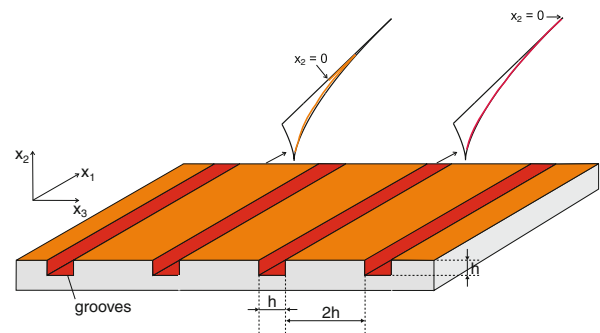


Fig. 2 Surface morphology capable of producing a smart interface between the flowing fluid and the solid boundary which promotes a large viscous drag reduction, but only under *particular* circumstances: microgrooves are inserted in the wall and are aligned in the flow direction with the aim of minimizing the energy dissipation rate ε by forcing fluctuations in the microgrooves toward the one-component limit. Sketched are the expected trajectories across anisotropy-invariant maps for each portion of the wetted surface

spectral energy transfer and, therefore, turbulence will never be initiated.

If we agree that the essential feature of turbulence is related to its ability to create motions at different scales and that the promotion of rapid mixing is caused by an increase in the spectral separation (which under common circumstances increases with increasing Reynolds number), then we should be able to stabilize the laminar boundary layer development by controlling only disturbances in the proximity of the wall. For a practical approach, this conclusion suggests that disturbances are forced to approach a one-component state at the wall. Since a similar forcing was applied in the previous work in fully developed turbulent channel flows and promising results were obtained with microgroove surface topology, it was decided to carry out similar experiments for laminar flow control.

The aim of this paper is to contribute toward an improved understanding of the fundamentals of laminar flow control by studying the stabilizing effect produced by surface-embedded microgrooves on the laminar boundary layer developing naturally along the front section of a two-dimensional channel. An experimental effort was made to provide the evidence for viscous drag reduction caused by a microgrooved surface morphology.

2 Experimental facility and measuring procedure

The two-dimensional channel and the related equipment that were used in the present experiments are similar to those employed in the previous investigations of flow control in fully developed turbulence (Frohnappel et al. 2007). The air flow was produced with a multi-purpose flow facility constructed according to DIN 24 163 (1985) requirements. It consists of a large circular housing 2.2 m in diameter and 7 m in length equipped with a centrifugal fan and a speed-controlled d.c. motor unit, a set of five Venturi nozzles manufactured according to DIN 1952 for determination of the volume flow rate, an assembly of honeycomb and screens and an outlet module which allows connection of the chamber housing to the experimental test section. This general-purpose facility provides well-controlled flow rates, good flow uniformity and a satisfactory turbulence level at the entrance of the experimental test section. Whereas a tripping device at the channel inlet ensured a fully developed turbulent state in the previous investigations, the channel was now equipped with a two-dimensional nozzle having a contraction ratio of 8:1 which was flush mounted with the channel top and bottom walls. The set-up thus provided natural development of boundary layers along the test section walls.

Two different arrangements of the test sections were used, one with flat walls and the other with microgroove-

modified walls, where a microgrooved surface was installed in the front part of the channel test section as shown in Fig. 3. To investigate the potential stabilizing effect of the microgrooved surface topology on the initial boundary layer development, a surface structure with microgroove dimensions $h = 150\ \mu\text{m}$ and separation $2h = 300\ \mu\text{m}$ was employed (see Fig. 2). The physical dimensions of the surface microgrooves were the same as used in the previous experiments on turbulent drag reduction. The surface pattern was produced by machine milling and mechanically polished after manufacture to eliminate irregularities in the surface pattern produced during the milling process.

To quantify the stabilizing effect of a structured surface which is expected to produce a decrease in pressure loss, measurements of pressure differentials were made along two channel test sections. A Scanivalve pressure scanner and a calibrated Höntzsch pressure transducer with a combined range of 0–1 kPa were used to for this propose with a resolution of 0.1% full-scale. Using different gain setting it was possible to obtain higher resolutions resulting in additional measuring ranges of 300, 100, 30, and 10 Pa full-scale. Special care was taken to maintain the transducer drift as small as possible, since this could produce significant measuring errors resulting in misleading conclusions. For all reported results, the drift was within 0.3% of full-scale deflection of the corresponding measuring range. The pressure signals were averaged over a period of 300 s, which was found to be sufficiently long to achieve good measuring accuracy at all Reynolds numbers.

To clarify the character of the transitional flow regime in the test section, preliminary measurements of turbulence were performed using hot-wire anemometry. These measurements were made at the channel centerline and very close to its exit by systematically increasing the flow rate, starting from the minimum up to the desired maximum value and subsequently by decreasing the volume flow rate from the maximum toward the minimum value. For naturally developing flow conditions, statistical quantities and the transition Reynolds number exhibit a large hysteresis effect, i.e. differences for increasing and decreasing flow rates (Fischer 1999). These differences can be clearly seen in Fig. 4 and suggest that laminar flow control experiments must be made consistently in the same fashion and with identical flow conditions at the channel inlet in order to obtain meaningful conclusions from the experimental results. Since it is well known that a delay of the breakdown leading to turbulence is far more easy to achieve for a low intensity of free stream turbulence, all experiments were performed by slowly increasing the flow rate in the channel.

Several hundred measurements were made in which a wide range of different parameters were explored. The flow conditions were successively refined until the optimum

Fig. 3 Two-dimensional channel flow with flat and microgroove-modified test section arrangements. **a** Reference test section configuration. **b** Configuration of the test section for laminar flow control

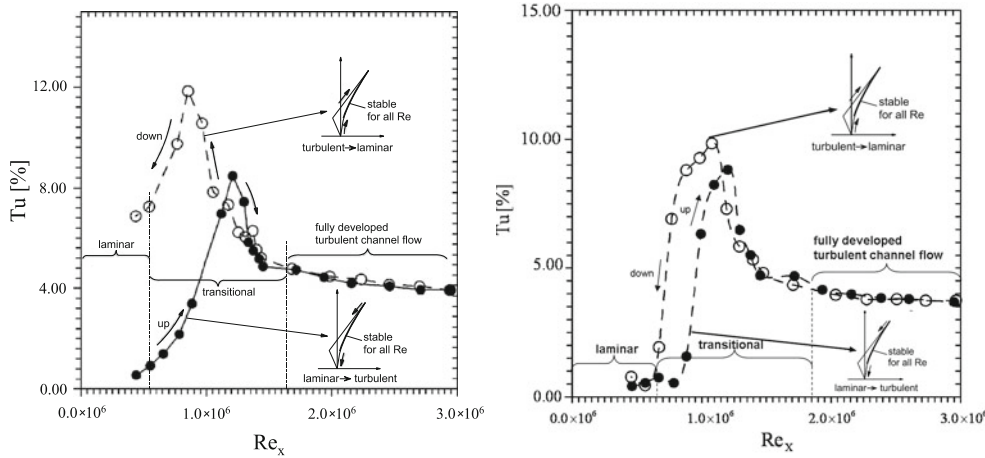
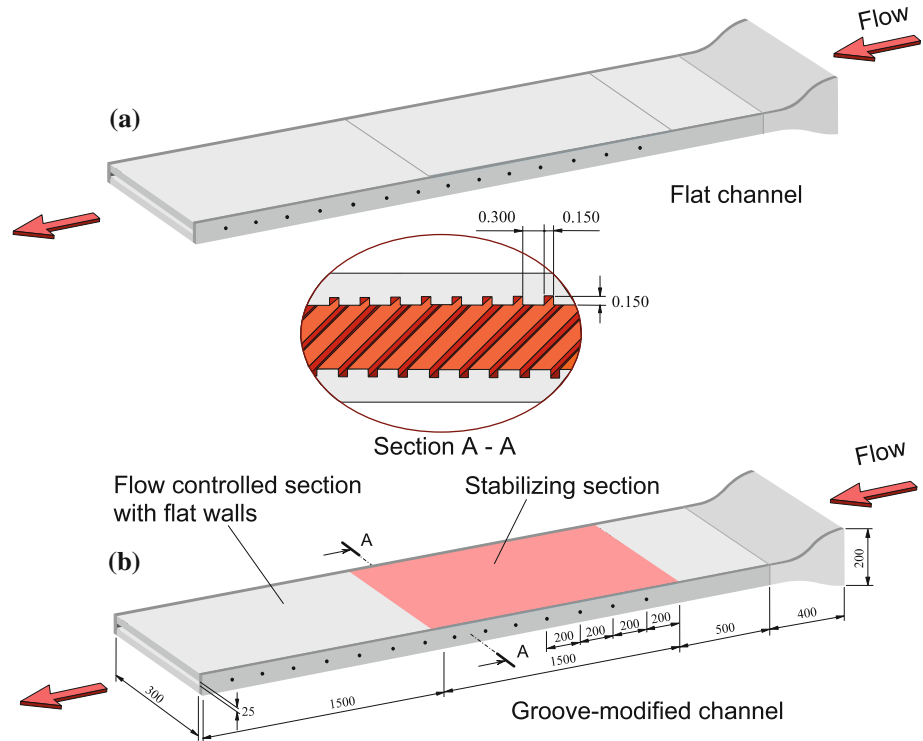


Fig. 4 Different faces of transition in a flat channel (left) and in the microgroove-modified channel (right): intensity of turbulence normalized by the mean velocity $Tu = \sqrt{u'^2}/\bar{U}_c$ measured at the channel centerline for increasing (filled circle) and decreasing (open circle)

flow rates as a function of the Reynolds number Re_x . The insets provide a possible interpretation of the experimental results in terms of anisotropy variations during forward and reverse transitions across the anisotropy-invariant map (Jovanović et al. 2006)

parameters for successful drag reduction measurements were achieved.

3 Experimental results

Experiments were conducted at channel bulk velocities between 2.3 and 11.8 ms^{-1} , corresponding to the Reynolds

number range¹ $Re_x = 0.5 \times 10^6 - 2.8 \times 10^6$. Since the experiments were conducted under developing flow conditions, the representative Reynolds number $Re_x = U_B L/\nu$ is based on the bulk velocity, U_B , the entire test section length, $L = 3.5 \text{ m}$, and the air viscosity, ν . The local

¹ The Reynolds number range based on the full channel height $H = 25 \text{ mm}$ was $Re_m = U_B H/\nu = Re_x H/L = 3.6 \times 10^3 - 20 \times 10^3$.

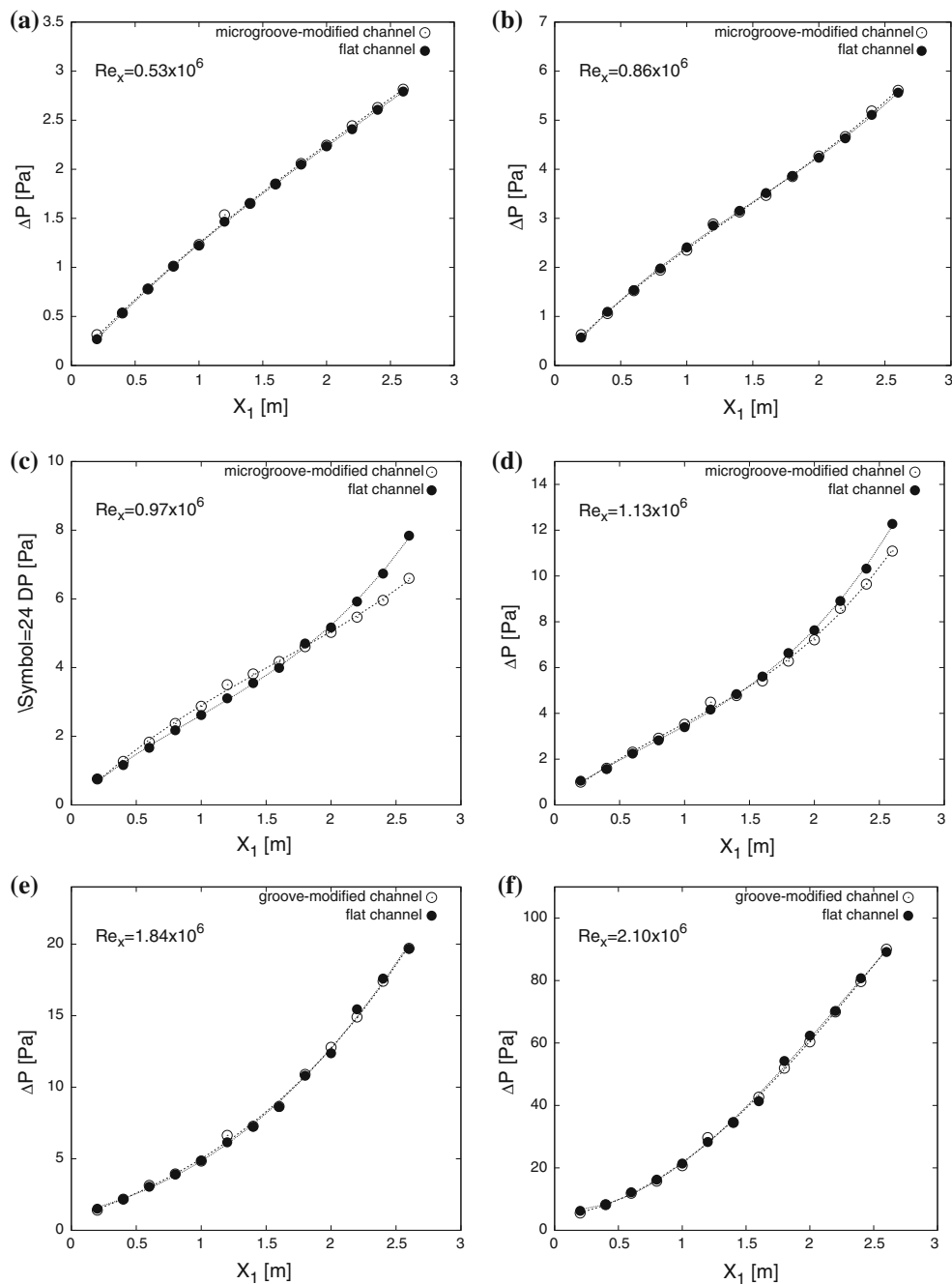


Fig. 5 Comparisons of pressure drop distributions measured over flat and microgroove-modified test sections at different Reynolds numbers. The Reynolds numbers are based on the bulk velocity and the test section length

pressure drop measurements along the flat and microgroove-modified test sections are presented as the difference with respect to the pressure measured at the first pressure tap located 0.7 m from the test section inlet as shown in Fig. 3.

For the microgroove-modified channel, the pressure drop measurements made at the first six points in the flow direction correspond to the front part of the channel test section where the structured surface was placed. The

following seven pressure measurements correspond to the rear part of the test section with smooth channel walls as shown in Fig. 3b.

The nonlinear variations in pressure drop distributions shown in Fig. 5a and b, which correspond to the laminar regime and relatively low Reynolds numbers, indicate that the flow is developing. From these distributions, it appears that in the laminar flow regime there is no noticeable difference in the pressure losses between flat and microgrooved

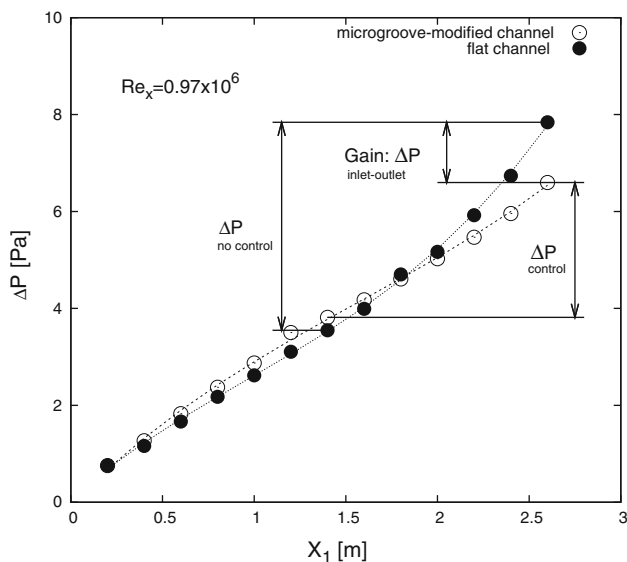


Fig. 6 Comparison of pressure drop distributions in flat and microgroove-modified test sections for maximum drag reduction effect

surfaces, suggesting that an increase in the wetted area has no impact on the viscous drag if the microgrooves are smaller than about 1.5 viscous length-scale (see Fig. 8).

In Fig. 5e and f, the pressure drop distributions approach a linear trend for the last few measuring stations, which indicates that the flow tends toward a fully developed state. It may be concluded by taking into account the results in Fig. 4 that the pressure drop measurements in the rear part correspond to the turbulent regime. Comparisons of these measurements carried out in flat and microgroove-modified test sections display no difference, implying that the microgrooved surface has no impact on the pressure loss if the microgroove dimensions are larger than about 2.5 viscous length-scales (see Fig. 8). These results are in fair agreement with our previous experiments made in a fully developed turbulent channel flow at low Reynolds numbers, in which a large turbulent drag reduction was measured only in a narrow range of flow velocities which corresponds to microgroove dimensions slightly smaller than one viscous length-scale (Frohnepfel et al. 2007).

Noticeable differences in the pressure drop measurements between flat and microgroove-modified test sections can be observed in the transitional regime as shown in Fig. 5c and d. In the front part of the test section (i.e. the first six measurement points in the flow direction), which consists of flat channel walls in the reference case and a microgrooved surface structure in the microgroove-modified channel, the pressure drop is slightly increased in the microgroove-modified test section. However, in the rear part of the test section, which consists of smooth channel walls in both cases, the pressure drop is reduced such that the pressure drop over the entire test section is smaller for

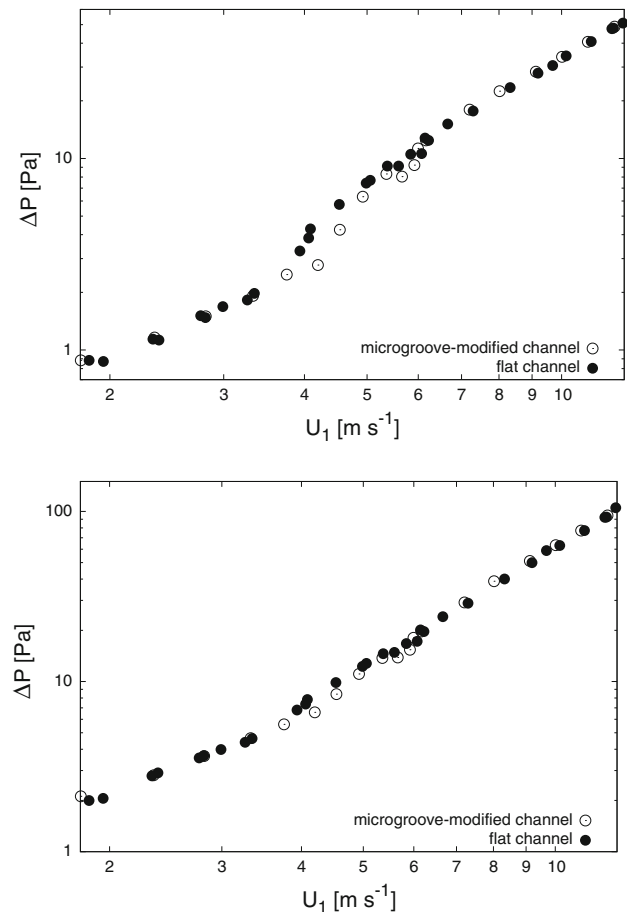


Fig. 7 The experimental data employed for estimation of viscous drag reduction. Comparisons of pressure drop measurements made over the rear part of the reference channel with flat walls with measurements made over the corresponding part of a microgroove-modified channel (*top*). Comparisons of pressure drop measurements made over the entire length of the reference channel with flat walls with corresponding measurements made in a microgroove-modified channel (*bottom*)

the microgroove-modified channel. The slightly increased pressure drop in the front part of the test section can be interpreted as interaction of microgroove structures with near-wall disturbances, which results in a stabilizing effect for the further flow development over the rear flat part of the channel. The results confirm indirectly the favorable action of the structured surface, which is designed to prevent the growth of disturbances very close to the wall. Figure 6 stresses the details of Fig. 5c and shows that maximum gain resulting in a large reduction of the pressure drop is achieved by stabilizing the boundary layer development over the rear flat part of the microgroove-modified test section.

On the basis of the theoretical considerations, it is expected that the structured surface as shown in Fig. 2 can effectively stabilize the laminar boundary layer development only under a relatively narrow range of flow

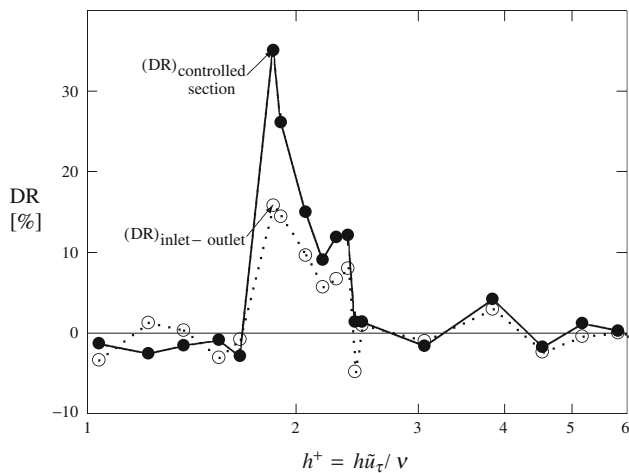


Fig. 8 Drag reduction versus nondimensional microgroove height: $(DR)_{\text{controlled section}}$, drag reduction measured over the flat part of the microgroove-modified test section; $(DR)_{\text{inlet-outlet}}$, net drag reduction measured over the entire length of the microgroove-modified test section

conditions. The experimental results shown in Fig. 5 support this conjecture and suggest that without attempting to vary the flow conditions in small steps, it is not possible to detect the regime for which microgrooves favorably influence viscous drag reduction (Bushnell et al. 1977).

By comparison of the pressure drop measured in the flat and microgroove-modified test sections, the drag reduction due to the stabilizing effect of the microgrooved surface on laminar boundary layer development can be estimated as follows:

$$DR = 1 - \frac{(\Delta p)_{\text{microgroove-modified channel}}}{(\Delta p)_{\text{flat channel}}} \tag{2}$$

The experimental data for the pressure drop along the channel test section and the bulk flow velocity employed for estimation of viscous drag reduction are presented in Fig. 7.

Figure 8 shows drag reduction results plotted against the dimensionless microgroove size according to

$$h^+ = \frac{\tilde{u}_\tau h}{\nu} \tag{3}$$

where the average value of the friction velocity, \tilde{u}_τ , was determined from the pressure drop measured over the front part of the test section and the cross-sectional area of the reference channel with smooth walls.

From the experimental results presented in Fig. 8, it appears that a high drag reduction was obtained in a narrow range of flow velocities which correspond to the dimensionless size of the microgrooves between 1.5 and 2.5 viscous length-scales. The trends in the experimental data reveal that the high drag reduction $DR \approx 35\%$ originates

from the decrease in the pressure drop over the rear flat portion of the microgroove-modified test section, resulting in an overall net gain of $DR \approx 16\%$. There is a strong similarity between the results presented here and those obtained in fully developed turbulent channel flow (Frohnapfel et al. 2007). This evidence is not accidental and indicates similarity in causative physics hidden behind the mechanism responsible for turbulent drag reduction and the mechanism capable of preventing breakdown of an initially laminar boundary layer leading to turbulence (Bushnell et al. 1977; Jovanović et al. 2006).

4 Conclusions and final remarks

To investigate the stabilizing effect of surface-embedded microgrooves on laminar boundary layer development, drag reduction experiments were conducted in the inlet region of a two-dimensional channel flow. By comparing pressure drop measurements made along flat and microgroove-modified test sections, the favorable influence of a microgrooved surface on viscous drag reduction was quantified by relatively simple means. A high drag reduction effect was found to persist in the range of flow velocities corresponding to microgroove dimensions between 1.5 and 2.5 viscous length-scales, which is wider than obtained previously in fully developed turbulent channel flow.

The experimental results obtained in this study provide interesting evidence of the similarity between turbulent drag reduction and laminar boundary layer control. In addition, they indirectly support the fundamental deductions that disturbances in the laminar boundary layer must be statistically axisymmetric and invariant under rotation about the axis aligned with the mean flow direction in close proximity to the solid boundary in order to ensure that the flow remains laminar during its development at very high Reynolds numbers (Jovanović et al. 2006).

Acknowledgments This work was sponsored by grants Jo 240/5-3, FR 2823/2-1 and in addition obtained support from the Cluster of Excellence Engineering of Advanced Materials at the University of Erlangen-Nuremberg and from the Center for Smart Interfaces at the Technische Universität Darmstadt, which are all funded by the German Research Foundation (DFG).

References

Bushnell DM, Hefner JN, Ash RL (1977) Effect of compliant wall motion on turbulent boundary layers. *Phys Fluids* 20(Part II): S31–S48
 DIN 24 163 (1985) Normenausschuß Maschinenbau (NAM), Teil 1, 2 und 3. Deutsches Institut für Normung e.V., Berlin
 Fischer M (1999) Turbulent wall-bounded flows at low Reynolds numbers (in German). PhD thesis, University Erlangen-Nuremberg, ibidem-Verlag, Stuttgart

- Frohnäpfel B, Jovanović J, Delgado A (2007) Experimental investigation of turbulent drag reduction by surface-embedded grooves. *J Fluid Mech* 590:107–116
- Frohnäpfel B, Lammers P, Jovanović J, Durst F (2007) Interpretation of the mechanism associated with turbulent drag reduction in terms of anisotropy invariants. *J Fluid Mech* 577:457–466
- Hinze JO (1975) *Turbulence*. 2nd edn. McGraw-Hill, New York
- Jovanović J, Frohnäpfel B, Škaljić E, Jovanović M (2006) Persistence of the laminar regime in a flat plate boundary layer at very high Reynolds number. *J Thermal Sci* 10:63–96
- Laufer J (1975) New trends in experimental turbulence research. *Annu Rev Fluid Mech* 7:307–326
- Laufer J (1982) Flow instability and turbulence. In: Zarić Z (ed) *Structure of turbulence in heat and mass transfer*. Hemisphere, pp 3–5
- Lee C, Kim J (2002) Control of the viscous sublayer for drag reduction. *Phys Fluids* 14:2523–2529
- Moser RD, Kim J, Mansour NN (1999) Direct numerical simulation of turbulent channel flow up to $Re_\tau = 590$. *Phys Fluids* 11:943–945
- Satake S, Kasagi N (1996) Turbulence control with a wall-adjacent thin layer of spanwise damping force. *Int J Heat Fluid Flow* 17:343–352